Astrophysics **Open Papers**, 1–7 (2014) Printed 5 August 2014 (My LaTeX style file v1.0)

Inversion of stellar parameters from high-resolution Echelle spectra

F. Paletou[1,2⋆], J.-F. Trouilhet[1,2] † and T. Böhm [2,1]‡
[1] *Université de Toulouse, UPS-Observatoire Midi-Pyrénées, Irap, Toulouse, France*
[2] *CNRS, Institut de Recherches en Astrophysique et Planétologie, 14 ave. E. Belin, F–31400 Toulouse, France*

arXiv:1401.1083v2 [astro-ph.IM] 4 Aug 2014

Please send us any comments etc..

ABSTRACT

The general context of this study is the inversion of stellar fundamental parameters from high-resolution Echelle spectra. We aim indeed at developing a fast and reliable tool for the post-processing of spectra produced by Espadons and Narval spectropolarimeters. Our inversion tool relies on principal component analysis. It allows reduction of dimensionality and the definition of a specific metric for the search of nearest neighbours between an observed spectrum and a set of synthetic spectra. Effective temperature, surface gravity, total metallicity and the projected rotational velocity are derived. Our first tests, done from the sole information coming from a spectral band very similar to the one the RVS spectrometer will observe from the Gaia space observatory, and with spectra mainly taken from FGK stars are very promising. We also tested our method with a few targets beyond this domain of the H–R diagram.

Key words: Methods: data analysis – Stars: fundamental parameters – Astronomical databases: miscellaneous

1 INTRODUCTION

This study is concerned with the inversion of fundamental stellar parameters from the analysis of high-resolution Echelle spectra. Hereafter, we shall focus indeed on data collected since 2006 with the Narval spectropolarimeter mounted at the 2-m aperture *Télescope Bernard Lyot* (TBL) telescope located at the summit of the *Pic du Midi de Bigorre* (France). We investigate, in particular, the capabilities of the principal component analysis (hereafter PCA) for setting-up a fast and reliable tool for the inversion of stellar fundamental parameters from these high-resolution spectra.

The inversion of stellar fundamental parameters for each target that was observed with both Narval and Espadons spectropolarimeters constitutes an essential step towards: *(i)* the further post-processing of the data like e.g., the extraction of polarimetric signals (see e.g., Paletou 2012) but also *(ii)* the exploration, or data mining, of the full set of data accumulated over the last 8 years now. In Section 2, we briefly describe the actual content of such a database.

PCA have been used for stellar spectral classification since Deeming (1964). It has been in use since, and more recently for the purpose of the *inversion* of stellar fundamental parameters from the analysis of spectra of various resolutions. It is however most often used *together* with artificial neural networks (see e.g., Bailer-Jones 2000; Re Fiorentin et al. 2007). PCA is used there for reducing the dimensionality of the spectra before attacking a multi-layer perceptron which, in turns, allows to link input data to stellar parameters.

Our usage of PCA for such an inversion process is strongly influenced by the one routinely made in *solar* spectropolarimetry during the last decade after the pionneering work of Rees et al. (2000). Very briefly, the reduction of dimensionality allowed by PCA is directly used for building a specific metric from which a nearest neighbour(s) search is done between an observed data set and a learning database. The latter is made of synthetic data generated from input parameters properly covering the *a priori* range of physical parameters expected to be deduced from the observations themselves. A quite similar use of PCA was also presented for classification and redshift of galaxies estimation by Cabanac et al. (2002). Fundamental elements of our method and its basic capabilities are exposed in Sections 3 and 4. One of its originality relies on the simultaneous inversion of the effective temperature $T_{\rm eff}$, the surface gravity $\log g$, the full metallicity [M/H] and the projected rotational velocity $vsini$.

In this study we restrict ourselves, on purpose, to the spectral domain that will be observed by the RVS spectrom-

⋆ E-mail: fpaletou@irap.omp.eu
† E-mail: jtrouilhet@irap.omp.eu
‡ E-mail: tboehm@irap.omp.eu

eter on-board the Gaia spacecraft (Katz et al. 2004). The RVS will finally operate in a spectral domain of the order of 847–871 nm (F. Thévenin, private communication). However, for our study we shall use the nominal spectral domain mentioned up to 2012 in the litterature and which covers the spectral domain 847–874 nm, at the vicinity of the Ca II infrared triplet. The pertinence of this choice for the further characterization of the observed stars was discussed by Munari (1999). This allows us to anticipate reasonable stellar parameter inversions for stars from B8 to M8, a very large range of spectral types similar to the actual content of our database.

The conditioning of observed spectra prior to their ingestion into our inversion tool is detailed in Section 5, and first tests made with solar spectra observed by reflection over the surface of the Moon are discussed in Section 6. Additional tests are also presented and discussed in Section 7, mainly for FGK-dwarf stars for which fundamental parameters are already available from the so-called Spocs catalogue (Valenti & Fisher 2005). We then briefly discuss preliminary tests using spectra from giant stars as well as hotter and cooler than FGK stars.

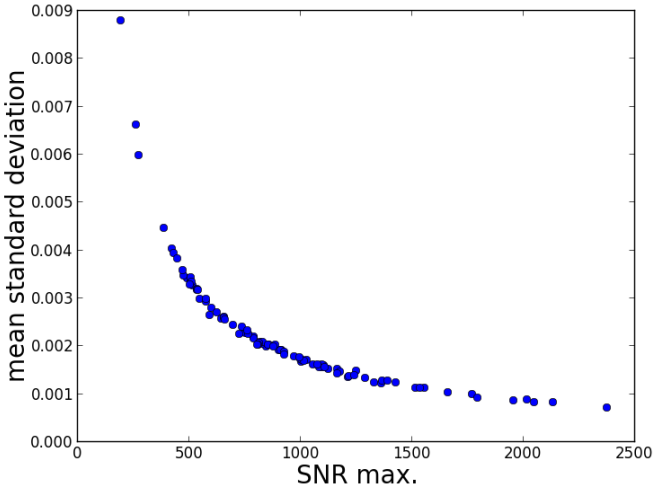

Figure 1. Typical domain of variation of the noise level associated with the Narval spectra we shall process. The standard deviation of noise per pixel, for the wavelength range around the infrared triplet of Ca II is displayed here vs. the maximum signal to noise ratio of the full spectra.

2 THE SOURCE OF DATA

We mainly used Narval data available from the *public* database TBLegacy[1]. Narval is a state-of-the-art spectropolarimeter operating in the 0.38-1 μm spectral domain, with a spectral resolution of 65 000 in its polarimetric mode. It is an improved copy, adapted to the 2-m TBL telescope, of the Espadons spectropolarimeter, in operations since 2004 at the 3.6-m aperture CFHT telescope.

The TBLegacy database is operational since 2007. It is at the present time the largest on-line archive of high-resolution polarization spectra. It hosts data that were taken at the 2-m TBL telescope since December 2006. So far, more than 70 000 spectra have been made available, for more than 370 distinct targets all over the Hertzsprung-Russell diagram. More than 13 000 *polarized* spectra are also available, mostly for *circular* polarization. Linear polarization data are very seldom still and amount to a few hundreds spectra, but they are equally available.

At the present time, the TBLegacy database provides no more than Stokes I or V/I_c spectra calibrated in wavelength. Stokes I data are either normalized to the local continuum or not. We have however plans: *(i)* to extend it to Espadons data from the CFHT telescope and *(ii)* to propose higher-level data, such as pseudo-profiles resulting from line addition and/or least-squares deconvolution (see e.g., Paletou 2012), activity indexes as well as stellar fundamentals parameters. The latter's knowledge, besides being obviously interesting by itself, is also indispensable to any accurate further post-processing of these high-resolution spectra. These spectra are also generally bearing high signal-to-noise ratios, as can be seen in Fig. (1). Indeed Stokes I spectra we have been using result from the combination of 4 successive exposures, each of them carrying 2 spectra of orthogonal polarities generated by a Savart plate-type analyser. This procedure of double so-called "beam-exchange" measurement is indeed meant for the purpose of extracting (very) weak polarization signals (see e.g., Semel et al. 1993).

[1] http://tblegacy.bagn.obs-mip.fr/ – note that one should rather use the more comprehensive `polarbase.irap.omp.eu` now

3 PCA INVERSION

Our PCA inversion tool is strongly inspired by magnetic and velocity field inversion tools which have been developed during the last decade to complement solar spectropolarimetry (see e.g., Rees et al. 2000). Improvements of this method have been recently exposed by Casini et al. (2013) for instance. Hereafter we describe its main characteristics, in the context of our study.

3.1 The training database

Let us call $\{S_i(\lambda)\}$ our training database of *synthetic* stellar spectra. Each of these spectra is characterised by a limited number of physical parameters which serve as input parameters for the numerical code producing them. Usually, for so-called *standard* stellar models, the minimal set of parameters is the effective temperature of the star, $T_{\rm eff}$, its surface gravity, log$g$, its *total* metallicity [M/H] (even though the specific iron abundance [Fe/H] is also frequently used) and a so-called microturbulent velocity ξ which is an artificial contributor to line widths, in addition to thermal (or Doppler) broadening.

Because a significant part of our database is constituted of moderately, say $vsini > 10\,{\rm km\,s^{-1}}$ to fast rotators, we adopted the collection of spectra already computed and made available by Munari et al. (2005). They used Castelli & Kurucz' Atlas code and they considered parameters spanning ranges from 3 500 K to 47 500 K for $T_{\rm eff}$, 0. to 5. for log$g$, -2.5 to 0.5 for [M/H], two distinct values, 0. and 0.4

for [α/Fe], microturbulent velocities ξ from 1 to 4 $\mathrm{km\,s^{-1}}$ and projected rotational velocities v*sini* ranging from 0 to 500 $\mathrm{km\,s^{-1}}$.

Our training database contains about 34 757 synthetic spectra after we limited ourselves to those spectra for which [α/Fe]=0, which may affect our determinations of [M/H] for some objects, and $\xi = 2\,\mathrm{km\,s^{-1}}$ which choice may also not be optimal for all of our observations. Also, only the so-called "new ODF" (where ODF stands for opacity distribution function; see Castelli & Kurucz 2003) spectra were selected for $T_{\rm eff} < 10\,000$ K. Hereafter we shall focus on the inversion of the set of four parameters $\{T_{\rm eff}$; log$g$; [M/H]; $vsini\}$ for each of our observed spectra.

It is also important to note that we used Munari et al. (2005) spectra computed for a resolving power of $\mathcal{R} = 20\,000$ i.e., about a factor of 3.25 *less* than the one of the observed spectra we want to process. We shall come back to this point in Sections 5 and 9.

3.2 Reduction of dimensionality

Each spectra from Espadons and Narval spectropolarimeters provides of the order of 250 000 flux measurements vs. wavelength across a spectral range spanning from 0.38 to 1 μm typically. Hereafter we consider only spectra obtained in the polarimetric mode at a resolvance $\mathcal{R} = 65\,000$. Indeed, one of our main objective is that stellar parameters derived from Stokes I spectra can be directly used for the further post-processing of the multi-line *polarized* spectra which comes together (see e.g., Paletou 2012 and references therein).

For this assessment study, we put ourselves on purpose in a tough situation by restricting the spectral domain from which we shall invert stellar parameters to the (initial) one of the RVS instrument of the Gaia space mission, that is for wavelengths ranging from about 847 to 874 nm (Katz et al. 2004). Arguments in favor of the use of this very spectral domain can also be found in Munari (1999). Considering this, the matrix $\vec{S}$ representing our training database turns to be $N_{\rm models} = 34\,757$ by $N_\lambda = 1\,569$.

Next we compute the eigenvectors $\vec{e}_k(\lambda)$ of the variance-covariance matrix defined as

$$\vec{C} = (\vec{S} - \bar{S})^T \cdot (\vec{S} - \bar{S})\,, \qquad (1)$$

where $\bar{S}$ is the mean of $\vec{S}$ along the $N_{\rm models}$-axis. Therefore $\vec{C}$ is a $N_\lambda \times N_\lambda$ matrix. In the framework of principal component analysis, reduction of dimensionality is achieved by representing the original data by a limited set of projection coefficients

$$p_{jk} = (S_j - \bar{S}) \cdot \vec{e}_k\,, \qquad (2)$$

with $k_{\rm max} \ll N_\lambda$. In what follows for the processing of all observed spectra, we shall adopt $k_{\rm max} = 14$.

The most frequent argument supporting the choice of $k_{\rm max}$ relies on the accuracy achieved for the reconstruction of the original set of S_i's from a limited set of eigenvectors (see e.g., Rees et al. 2000 or Ramírez Vélez et al. 2010). In the present case, we display in Fig. (2) the maximum reconstruction error

$$E(k_{\rm max}) = \max_j \left(\frac{\mid \bar{S} + \sum_{k=1}^{k_{\rm max}} p_{jk}\vec{e}_k - S_j \mid}{S_j} \right)\,, \qquad (3)$$

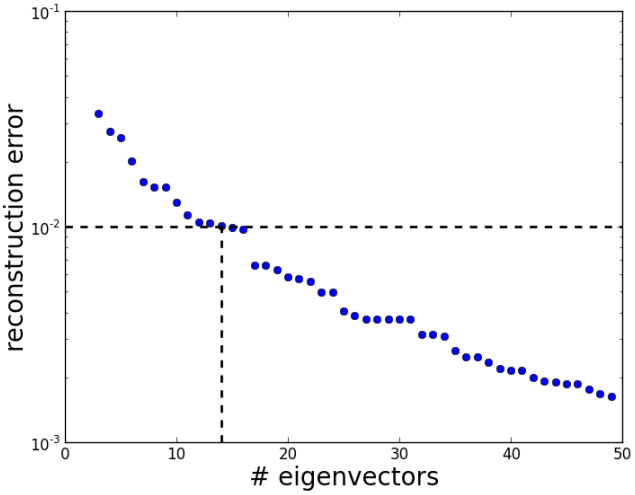

Figure 2. Reconstruction error as a function of the number of eigenvectors used for the computation of the admixture coefficients p.

as a function of the maximum number of eigenvectors considered for the computation of the so-called *admixture* coefficients p. It is noticeable that this reconstruction error is better than 1% for $k_{\rm max} \geqslant 14$. However the potentiel effect of noise present in the observations we want to process should also be taken into account (see e.g., Socas-Navarro et al. 2001). We shall discuss this specific point in the next Section.

Practically, we also found convenient to use, at every k order, p_{jk}'s both centered to their average $\bar{p}^{(k)}$ and normalized to their standard deviation $\sigma_p^{(k)}$. It is a common practice in the field of pattern recognition, since it guarantees that those coefficients from which we shall define the specific metric used for the nearest neighbour(s) search will have comparable effects (on the comparison between spectra).

3.3 Nearest neighbour(s) search

The above described reduction of dimensionality allows one to perform a fast and reliable inversion of observed spectra, once the latter have been: *(i)* corrected for the wavelength shift vs. synthetic spectra because of the radial velocity of the target, *(ii)* continuum-renormalized as accurately as possible, *(iii)* degraded in spectral resolution to be comparable to the $\mathcal{R} = 20\,000$ of the synthetic spectra and, finally *(iv)* resampled in wavelength as the collection of synthetic spectra. We shall come back to these various stages in the next section. However once these tasks have been achieved, the inversion process is the following.

Let $O(\lambda)$ the observed spectrum made comparable to synthetic ones. We now compute the reduced set of projection coefficients

$$\varrho_k = \frac{(O - \bar{S}) \cdot \vec{e}_k - \bar{p}^{(k)}}{\sigma_p^{(k)}}\,, \qquad (4)$$

where $\bar{p}^{(k)}$ and $\sigma_p^{(k)}$ are, respectively, the mean of the standard deviation of the p_{jk}'s, for $k = 1, \ldots, k_{\rm max}$. The nearest

Table 1. Standard deviation of the absolute differences between input and inverted parameters for noisy spectra vs. a (gaussian) white-noise level characterized by a $\sigma_{\rm noise}$ per pixel standard deviation.

$\sigma_{\rm noise}$	$\Delta T_{\rm eff}$ [K]	$\Delta\log g$	Δ [M/H]	$\Delta vsini\,[{\rm km\,s^{-1}}]$
0.05	200	0.52	0.21	15
0.02	101	0.27	0.10	5.5
0.01	46	0.12	0.04	2.6
0.005	10	0.04	0.01	0.5

neighbour search is therefore done by seeking the minimum of the squared *Euclidian* distance

$$d_j^{(O)} = \sum_{k=1}^{k_{\rm max}} \left(\varrho_k - p_{jk}\right)^2 \ , \tag{5}$$

where j spans the number, or a limited number if any *a priori* is known about the target, of distinct synthetic spectra in the training database. In practice, we do not limit ourselves to the nearest neighbour search, although it already provides a relevant set of stellar parameters. Because PCA-distances between several neighbours may be of the same order, we adopted a procedure which consists in considering *all* neighbours in a domain

$$\min\left(d_j^{(O)}\right) \leqslant d_j^{(O)} \leqslant 1.2 \times \min\left(d_j^{(O)}\right) \ , \tag{6}$$

and derive stellar parameters as the (simple) mean of each set of parameters $\{T_{\rm eff};\ \log g;\ [{\rm M/H}];\ vsini\}$ characterising this set of nearest neighbours (A. López Ariste, private communication). We did not notice significant changes in the results either for a smaller range of PCA-distances or when adopting e.g., distance-weighted mean parameters.

4 THE EFFECT OF NOISE ON THE INVERSION PROCESS

Before processing any real observed spectra with our PCA-based inversion tool, we need to investigate on the potential effect of noise. To do so, we have ingested in our inversion tool multiple realisations of the content of the very learning database $S_i(\lambda)$ affected by controlled (gaussian) white noise-levels, and we estimated how it affects the inversion process by systematically comparing (known) input and inverted parameters.

A first test was to check upon the choice of $k_{\rm max} = 14$ besides the argument already mentioned concerning the maximum reconstruction error. In fact, for noise levels characterized by a standard deviation per pixel better or equal to $\sigma_{\rm noise} = 0.01$ – see also Fig. (1) – internal errors are quite similar and minimal in the $k_{\rm max} \sim 12 - 15$ range. Typical values for each stellar parameter are given in Table 1. We could also check that these values start to significantly increase for values $k_{\rm max} \geqslant 16$, which confirmed to us the optimal choice of $k_{\rm max} = 14$ we made for the remainder of this study.

Results of the numerical experiments we summarized in Table 1 also describe the effect of signal to noise ratio on the quality of our inversion process. We did not notice any significant bias so that our values can also be compared to "mean maximum errors" used in other studies (e.g., Recio-Blanco et al. 2006 or Katz et al. 1998). It is also worth mentioning that, for increasing signal-to-noise ratio (i.e., decreasing value of $\sigma_{\rm noise}$) although we computed standard deviations on the distribution of the absolute errors between input and inverted parameters, these distributions of errors showed to be strongly skewed towards 0 and departing from gaussian. Finally, internal errors are about a factor of 2 better, if one limits the domain of work to $4000 \leqslant T_{\rm eff} \leqslant 7000$ K, $\log g \geqslant 3.0$ dex and $[{\rm M/H}] \geqslant -1.0$ dex according to the domain of parameters relevant for the Spocs–Narval targets we analysed in this study.

5 CONDITIONING OF THE OBSERVED SPECTRA

The first and obvious task to perform on *observed* spectra is to correct for their wavelength shift vs. synthetic spectra computed at radial velocity $V_{\rm rad} = 0$. The radial velocity of the target at the time of the observation is deduced from the centroid, in a velocity space, of the pseudo-profile resulting from the "addition" (see e.g., Paletou 2012) of the three spectral lines of the Ca II infrared triplet whose rest wavelengths are, respectively, 849.802, 854.209 and 866.214 nm. Once $V_{\rm rad}$ is known the observed profile is set on a new wavelength grid, at rest. We could check, using solar spectra (see §6.) that $V_{\rm rad}$ should be known to an accuracy of the order of $\delta v/3$ with $\delta v = c/\mathcal{R}$ i.e., in our case about 1.5 ${\rm km\,s^{-1}}$. Beyond this value, estimates of $vsini$ and, to a minor extent $T_{\rm eff}$, start to be significantly affected by the misalignement of the observed spectral lines with those of the synthetic spectra of the training database.

A second step consists in degrading the resolution of the initial spectra to the one of the synthetic spectra computed for $\mathcal{R} = 20\,000$. This is done by convolving the initial observed profile by a Gaussian profile of adequate width. Then we resample the wavelength grid down to the one common to all synthetic spectra, and we interpolate the original spectra onto the new wavelength grid.

Finally, we have to correct for unproper normalization of the Stokes I flux to the local continuum. This issue has been very well discussed in Gazzano et al. (2010) as well as in Kordopatis et al. (2011), and we adopted their iterative procedure. For the FGK stars spectra we have been mainly dealing with hereafter, we report no more than 3.5% initial relative error in position for the continuum level, while in most case this does not exceed 2%. The iterative correction procedure allows to renormalize our observed spectra at 10^{-4}, using successive estimates of the nearest neighbour synthetic spectra as a reference. This procedure is clearly required, and we also report on possible errors of the order of $\Delta T_{\rm eff} \sim 150$ K, $\Delta\log g \sim 0.1$ dex and $\Delta[{\rm M/H}] \sim 0.1$ dex due to unproper normalization of the continuum.

6 FIRST TESTS WITH OBSERVED SOLAR SPECTRA

First tests of our inversion method with real data were performed using solar spectra observed by the 2-m aperture

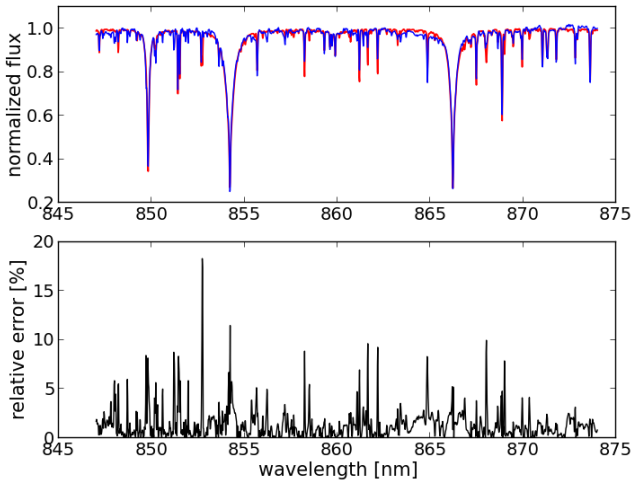

Figure 3. The top figure displays normalized flux from the observation of the Sun by reflection over the Moon made at the TBL with the Narval spectropolarimeter (blue) and the nearest PCA-distance synthetic spectrum (red). The latter corresponds to stellar parameters $T_{\rm eff}$=6000 K, log$g$=4.5, [M/H]=0 and $vsini$=5 km s^{-1}. The bottom figure displays the relative error vs. wavelength between the two spectra.

TBL telescope by reflection over the surface of the Moon in March and June 2012.

The synthetic spectrum having the minimal PCA-distance with the observed spectrum have model parameters $T_{\rm eff}$=6000 K, log$g$=4.5, [M/H]=0 and $vsini$=5 km s^{-1}. It is displayed against one of our observed spectra in Fig. (3). These values slightly overestimate "canonical" values of $T_{\rm eff}$=5780 K, log$g$=4.4 and $vsini$ about 2 km s^{-1} (see e.g., Pavlenko et al. 2012). However, considering the "bulk" of nearest neighbours in the range defined by inequalities (6), we derive more accurate parameters such as $T_{\rm eff}$=5772 K, log$g$=4.26, [M/H]=0 and $vsini$=2.2 km s^{-1}. Typically of the order of 20 neighbour-models are identified with our procedure and for Narval solar spectra.

The relevance of the PCA-distance on which rely our inversion process can also be verified by the examination of the characteristics of the set of nearest neighbours we could identify. In the solar spectrum case, we find: 9 models bearing $T_{\rm eff}$=5750 K, 6 models with $T_{\rm eff}$=5500 K, as many at 6000 K and one at 6250 K. For the surface gravity we find: 9 with log$g$=4.0, 6 with 3.5, as many at 4.5 and just one at 5.0. Finally, concerning the projected rotational velocity, we find: 8 models at 0, 7 at 2 km s^{-1} and as many at 5 km s^{-1}. Note finally that *all* neighbours have a solar metallicity [M/H]=0. From this point of view, it seems that we are doing better than Kordopatis et al. (2011) who state that they do not recover a metallicity better than -0.1 dex for a solar spectra using their pipeline combining the Matisse (projection) method (Recio-Blanco et al. 2006) and a kd-tree classification scheme.

7 OTHER FGK STARS

Because one of the originality of our inversion tool is in providing the projected rotational velocity of stars, we also tested its capability for a couple of FGK stars with significant ($\sim 15-20$ km s^{-1}) $vsini$ and belonging the so-called "Stellar properties of observed cool stars" (aka. Spocs) catalogue (Valenti & Fischer 2005).

For a first test, we used a spectra from the pre-main sequence star HD377 and comparison between Spocs parameters and ours are detailed in Table 2. Unfortunately, according to the Pastel catalogue (Soubiran et al. 2010) there are almost no alternative values given in the litterature for this object. Its $vsini$ is well recovered and other parameters agree reasonably well with Spocs values. Our second target is τ Boo (A, also HD120136), a F6IV star for which the Spocs catalogue provides a $vsini$ of 15 km s^{-1} while our estimate is about 19 km s^{-1}. However a $vsini$ of about 18 km s^{-1} has been recently reported by Martínez-Arnáiz et al. (2010). Other parameters agree very well, except for log$g$ that we systematically overestimated for these two objects.

A first excursion away from the FGK-dwarfs domain consists in exploring the luminosity class towards the giants domain. The red giant branch (G5) star HD12328 have been used for that purpose. Our results are again reliable given also that recent works mention an effective temperature of 4808 K, in better agreement with ours (Massarotti et al. 2008), as well as log$g$ value of the order of 3.3 dex and [Fe/H]=-0.04 dex (see also Jones et al. 2011). Outside the Spocs catalogue, and again for (sub-)giants, we also used data from the K1.5III star Arcturus. Our 4250 K determination of its effective temperature is very close, within 30 K, to that of Prugniel et al. (2011) for instance. We could also derive a surface gravity about 2.0 in agreement with alternative estimates (e.g., Massarotti et al. 2008) and our [M/H] and $vsini$ values are also in pretty well identified ranges, as reported in Table 2. Note that further tests with Pollux (K0III) data also gave excellent results. Concerning these classes of stars, we are also perfectly aware that additional synthetic spectra with microturbulent velocities not restricted to 2 km s^{-1} as we did here, will have to be next considered. Note also that for (sub-)giant stars, models computed in (1D) *spherical* geometry such as MARCS ones (Gustafsson et al. 2008) may also provide a more realistic description of the observed stellar fluxes and therefore improve the determination of the inverted stellar parameters.

8 BEYOND THE FGK DOMAIN

Our database of spectropolarimetric data already covers pretty well the H-R diagram. We are therefore interested in spanning most of it, and basically with the same inversion tool. Selected targets for these further tests are indicated, together with the parameters we derived from their spectra, in Table 2.

For cooler stars, we picked spectra of GL 205, a M1.5V dwarf. Our values of $T_{\rm eff}$, log$g$ and [M/H] agree very well with those of Prugniel et al. (2011), and our $vsini$ determination agrees well with the one of Houdebine (2010). There is also a reasonable agreement with values recently derived by Neves et al. (2013).

Table 2. Summary of the comparison between our inverted parameters and these provided: (1) by the Spocs catalogue and (2) in the litterature i.e., using Simbad at CDS and/or the Pastel catalogue (Soubiran et al. 2010), for the objects listed below.

Object	$T_{\rm eff}^{\rm (Spocs)}$	$T_{\rm eff}^{\rm (PCA)}$	log$g^{\rm (Spocs)}$	log$g^{\rm (PCA)}$	[M/H]$^{\rm (Spocs)}$	[M/H]$^{\rm (PCA)}$	$vsini^{\rm (Spocs)}$	$vsini^{\rm (PCA)}$
HD 377	5873	5644	4.3	4.70	0.1	0.0	14.6	15.2
HD 120136	6387	6366	4.3	4.68	0.2	0.2	15.0	19.3
HD 12328	4919	4761	3.7	3.63	-0.1	-0.03	1.9	2.6
Object	$T_{\rm eff}^{\rm (Litt.)}$	$T_{\rm eff}^{\rm (PCA)}$	log$g^{\rm (Litt.)}$	log$g^{\rm (PCA)}$	[M/H]$^{\rm (Litt.)}$	[M/H]$^{\rm (PCA)}$	$vsini^{\rm (Litt.)}$	$vsini^{\rm (PCA)}$
GL 205	3 730	3 750	4.73	4.8	0.0	0.0	2.73	3.
Arcturus	4 290	4 250	1.7	2.0	-0.5	-0.5	4.2	5.
Sirius	9 830	10 500	4.3	4.5	0.34	0.5	16.	20.

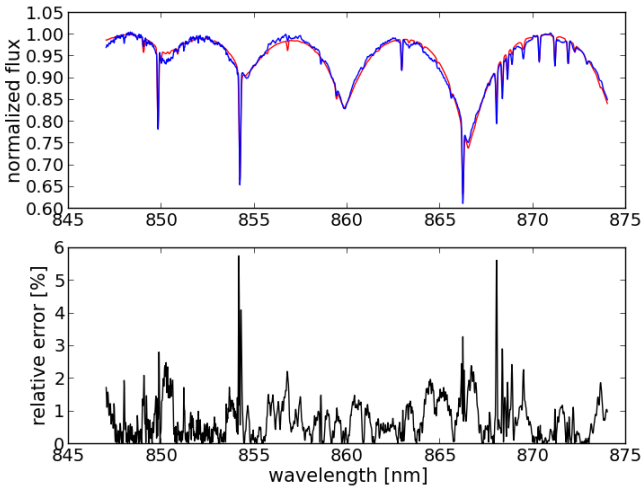

Figure 4. Same as Fig. (3) but for Sirius A.

Finally, we also tested our method with spectra of the A1V star Sirius (A). Our inversion of the effective temperature gives a value a bit larger than the 9870 K more recently reported (Hill & Landstreet 1993). [M/H] is also overestimated, but log$g$ and *vsini* are quite well determined. We are also aware that, so far, we restricted ourselves to models such that [α/Fe]=0 which may not apply to such a star. Possible enhancement of α-elements will be considered in a next version of our inversion tool, when performing spectral analysis at a larger scale than the one presented here. However, besides this current restriction, the agreement between the observed spectrum and the nearest neighbour synthetic spectrum is already quite satisfactory, as shown in Fig. (4).

9 DISCUSSION

Concerning the determination of *vsini*, other methods of evaluation exist. However, to the best of our knowledge, they always require a template spectrum or at least a list of spectral line *a priori* expected in the spectra, as auxilliary and "support" data (see e.g., Díaz et al. 2012 and references therein). Our final pipeline will therefore implement an additional module providing, once a preliminary stellar parameter inversion will be available from our inversion tool, an alternative and complementary *vsini* evaluation. Note also that, with our PCA method, we are mostly interested in the "intermediate" *vsini* regimes, say between 10 and 100 km s^{-1}. Indeed, for slow rotators it is obvious that rotational broadening becomes of the order of other sources of broadening (e.g., instrumental or turbulent) so that a more detailed line profile analysis may be required. On the other hand, (very) fast rotators are affected by macroscopic effects such as gravity darkening (see e.g., Espinosa Lara & Rieutord 2011) which are not accounted for, so far, by standard atmospheric (radiative) modelling.

Another source of potential improvement relies on the content of our learning database. ATLAS standard models may not be the best choice for cool stars or for metal-poor stars for instance. It is also well-known that non-LTE effects may take place in the formation of the infrared triplet of Ca II, which affects the spectral lines central depressions. This issue was for instance mentioned in Kordopatis et al. (2011). More detailed elements, from the point of view of radiative modelling, are also discusses in Merle et al. (2011). Finally, we shall need synthetic spectra computed for a resolvance comparable to the one of our observations and, ideally, including the effects of rotational broadening. The database of synthetic spectra, Pollux (Palacios et al. 2010) already provides a partial answer to our needs, and we believe that its development will take into account such needs.

10 CONCLUSION

We have experimented a fast and reliable PCA-based numerical method for the inversion of stellar fundamental parameters $T_{\rm eff}$, log$g$ and [M/H], as well as the projected rotational velocity *vsini*, from high-spectral resolution Echelle spectra taken from the Narval spectropolarimeter in operations at the 2-m TBL telescope.

Our method is fast and easy to implement. First tests, mainly made for FGK-stars spectra show fairly good agreement with reference values published by Valenti & Fischer (2005). Preliminary tests also suggest that the same method is applicable to FGK (sub-)giants, as well as to cooler M stars or hotter stars up to spectral type A. We used it, so far, at the vicinity of the infrared triplet of Ca II and without any help from additional (e.g., photometric) information, which is particularly challenging. However we can easily, either extend the spectral domain used by our inversion method, or combine analyses from several distinct spectral domains, in

order to constrain further and refine our stellar parameter determination.

It is finally important to realize from the present study that PCA allows for a reduction of dimensionality of the order of 100 ($\sim N_\lambda/k_{\max}$) which is of great potential interest for the post-processing of high-resolution spectra covering a very large bandwidth like the ones from both Espadons and Narval spectropolarimeters.

ACKNOWLEDGMENTS

We are grateful to Dr. Tomaz Zwitter (University of Ljubljana, Slovenia) who made available the synthetic spectra used in the work. This research has made use of the VizieR catalogue access tool, CDS, Strasbourg, France. The original description of the VizieR service was published in A&AS 143, 23. This research has made use of the SIMBAD database, operated at CDS, Strasbourg, France. Narval data were provided by the OV-GSO datacenter operated by CNRS/INSU and the *Université Paul Sabatier, Toulouse*-OMP (Tarbes, France; `polarbase.irap.omp.eu`).

REFERENCES

Bailer-Jones, C.A.L. 2000, ApJ, 357, 197
Cabanac, R.A., de Lapparent, V., Hickson, P. 2002, A&A, 389, 1090
Casini, R., Asensio Ramos, A., Lites, B. W., López Ariste, A. 2013, ApJ, 773, 180
Castelli, F., Kurucz, R.L. 2003, in IAU Symp. No 210, Modelling of Stellar Atmospheres, eds. N. Piskunov et al., poster A20 [arXiv:astro-ph/0405087]
Deeming, T.J. 1964, MNRAS, 127, 493
Díaz, C.G., González, J.F., Levato, H., Grosso, M. 2011, A&A, 531, A143
Espinosa Lara, F., Rieutord, M. 2011, A&A, 533, 43
Gazzano, J.-C., de Laverny, P., Deleuil, M., et al. 2010, A&A, 523, 91
Gustafsson, B., Edvardsson, B., Eriksson, K., Jørgensen, U.G., Nordlund, Å, Plez, B. 2008, A&A, 486, 951
Hill, G.M., Landstreet, J.D. 1993, A&A, 276, 142
Houdebine, E. 2010, MNRAS, 407, 1657
Jones, M.I., Jenkins, J.S., Rojo, P., Melo, C.H.F. 2011, A&A, 536, 71
Katz, D., Munari, U., Cropper, M., et al. 2004, MNRAS, 354, 1223
Katz, D., Soubiran, C., Cayrel, R., Adda, M., Cautain, R. 1998, A&A, 338, 151
Kordopatis, G., Recio-Blanco, A., de Laverny, P., et al. 2011, A&A, 535, 107
Martínez-Arnáiz, R., Maldonado, J., Montes, D., Eiroa, C., Montesinos, B. 2010, A&A, 520, 79
Massarotti, A., Latham, D.W., Stefanik, R.P., Fogel, J. 2008, AJ, 135, 209
Merle, T., Thévenin, F., Pichon, B., Bigot, L. 2011, MNRAS, 418, 863
Munari, U. 1999, Baltic Astron., 8, 73
Munari, U., Sordo, R., Castelli, F., Zwitter, T. 2005, A&A, 442, 1127
Neves, V., Bonfils, X., Santos, N.C., et al. 2013, A&A, 551, A36
Palacios, A., Gebran, M., Josselin, E., et al. 2010, A&A, 516, A13
Paletou, F. 2012, A&A, 544, 4
Pavlenko, Ya V., Jenkins, J.S., Jones, H.R.A., Ivanyuk, O., Pinfield, D.J. 2012, MNRAS, 422, 542
Prugniel, P., Vauglin, I., Koleva, M. 2011, A&A, 531, A165
Ramírez Vélez, J. C., Semel, M., Stift, et al. 2010, A&A, 512, 6
Recio-Blanco, A., Bijaoui, A., de Laverny, P. 2006, MNRAS, 370, 141
Rees, D.E., López Ariste, A., Thatcher, J., Semel, M. 2000, A&A, 355, 759
Re Fiorentin, P., Bailer-Jones, C.A.L., Lee, Y.S, et al. 2007, A&A, 465, 1373
Semel, M., Donati, J.F., Rees, D.E. 1993, A&A, 278, 231
Socas-Navarro, H., López Ariste, A., Lites, B.W. 2001, ApJ, 553, 949
Soubiran, C., Le Campion, J.-F., Cayrel de Strobel, G., Caillo, A. 2010, A&A, 515, 111
Valenti, J.A., Fischer, D.A. 2005, ApJS, 159, 141